**Astronomy & Astrophysics**

# $H_3^+$ and other species in the diffuse cloud towards $\zeta$ Persei: A new detailed model

F. Le Petit[1,2], E. Roueff[1], and E. Herbst[3]

[1] Observatoire de Paris-Meudon, LUTH, 5 place Jules Janssen, 92190 Meudon, France
[2] Onsala Space Observatory, 439 92 Onsala, Sweden
[3] Departments of Physics, Chemistry, and Astronomy, The Ohio State University, Columbus, OH 43210, USA

**Abstract.** McCall et al. have recently shown that a large column density for the molecular ion $H_3^+$ of $\approx 8 \times 10^{13}$ cm$^{-2}$ exists in the classical diffuse cloud towards $\zeta$ Persei. They have used this observation to infer that the cosmic ray ionization rate $\zeta$ for this source is approximately 40 times larger than previously assumed. But, although the value of $\zeta$ they infer ($\approx 1.2 \times 10^{-15}$ s$^{-1}$) can explain the abundance of $H_3^+$, it is not at all clear that such a high ionization rate is consistent with the many other detailed atomic and molecular observations made along the same line of sight. In particular, the abundances of the species OH and HD were previously used to determine a much lower ionization rate. In this paper, we report a detailed chemical model of the diffuse cloud towards $\zeta$ Persei which appears to fit to a reasonable extent both the older atomic and molecular observations and the new detection of $H_3^+$. We consider two phases – a long (4 pc) diffuse region at 60 K and a tiny ($\approx 100$ AU) dense region at 20 K, both with an ionization rate $\zeta$ in between the standard value and that advocated by McCall et al. The model reproduces almost all abundances, including that of $H_3^+$, to within a factor of three or better. To reproduce the CH$^+$ abundance and those of the excited rotational populations of $H_2$, we consider the addition of shocks. This phase has little effect on our calculated abundance for $H_3^+$.

**Key words.** molecular processes – ISM: cosmic rays – ISM: abundances – ISM: molecules – ISM: general

## 1. Introduction

The molecular ion $H_3^+$ plays a critical role in the ion-molecule chemistry of dense interstellar clouds. Produced by the cosmic ray ionization of molecular hydrogen followed by the reaction of $H_2^+$ and $H_2$, $H_3^+$ is a precursor for the production of many different molecular species (Herbst 2000). The inability to detect it for many years raised the possibility that the entire ion-molecule picture of interstellar chemistry might be in error. After many years of searching, Geballe & Oka (1996) finally detected this ion. Subsequent observations confirmed that the abundance of $H_3^+$ in dense clouds is in excellent agreement with the predictions of gas-phase chemical models (McCall et al. 1999). The relief of astrochemists was short-lived, however, because in 1999, Geballe et al. (1999) detected surprisingly large abundances of $H_3^+$ towards Cygnus OB2 No. 12, a complex line of sight that could reasonably be labelled as diffuse, as well as two similar sources in the Galactic Center. Indeed, the column density of $H_3^+$ detected is similar to that seen in dense clouds! This value is contradictory to predictions, based on models with a high rate of removal of $H_3^+$ by recombination with electrons. The rate coefficient for $H_3^+ + e^-$ has gone

through a complex history of assorted measurements; however, the dominant view now is that it is large – see below.

Although Geballe et al. (1999) raised the possibility that the diffuse material extends throughout much of the path between the star and earth, two other explanations for the high column density of $H_3^+$ soon emerged. Cecchi-Pestellini & Dalgarno (2000) suggested that the line of sight to Cygnus OB2 No. 12 is clumpy with pockets of inhomogeneous material at densities of $\approx 100$ cm$^{-3}$ and higher embedded in a wispy medium. The total visual extinction is 10.2 mag, arising from the combined effects of nine spherical clumps, while the ionization rate $\zeta$ is $6 \times 10^{-17}$ s$^{-1}$, somewhat higher than usual. Such pockets appear to explain the high abundance of $H_3^+$ as well as the observed abundances of the species $C_2$ and CO along the line of sight. Another suggestion, made by Black (2000), is that an unusually high ionization rate pertains due to X-rays. Interestingly, a high ionization rate, but due to 2 MeV cosmic rays, had been considered in the early days of molecular astronomy (Solomon & Werner 1971; Dalgarno & McCray 1972). Herbst & Klemperer (1973), in their initial model of dense cloud chemistry, had assumed $\zeta$ to be $\approx 10^{-15}$ s$^{-1}$ based on the work of Solomon & Werner (1971), but found the penetration depth of the low energy cosmic rays to be too small to affect dense cloud chemistry. Never a dominant view, the suggestion of a high ionization rate faded particularly when detailed studies of the OH and

HD abundances in classical diffuse clouds indicated a much lower ionization rate of $\approx 10^{-17}$ s$^{-1}$. With a high ionization rate and an elemental D/H ratio near $10^{-5}$, it was thought that both of these species would be significantly overproduced in chemical models at diffuse cloud temperatures (Hartquist et al. 1978) but, as will be shown later, this result is quite temperature sensitive.
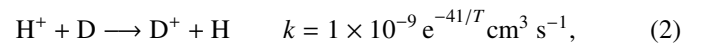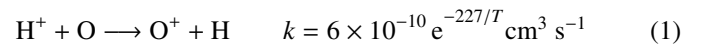
Subsequent observations of large amounts of $H_3^+$ in the directions of a variety of quasi-diffuse sources soon followed the original detections (McCall et al. 2002). These observations did not serve to determine the relative importance of a long path length, a high ionization rate, or clumpy material in producing a large amount of the ion. Indeed, the explanation in terms of a small value for the dissociative rate coefficient for the reaction between $H_3^+$ and electrons still has some if not dominant experimental support (Plasil et al. 2003). This viewpoint is a minority one because of a variety of experiments that show the opposite, including the initial discharge work of Amano (1988) and the subsequent storage-ring work of Larsson and collaborators (Larsson et al. 1993; Larsson 2000). The most recent measurements by McCall et al. (2003) using a thermal source in a storage ring confirm a reasonably large rate coefficient for the $H_3^+$ dissociative recombination, and are in agreement with new theoretical results (Kokoouline & Greene 2003).

In the same paper that announced the new storage-ring measurements, McCall et al. (2003) announced the detection of $H_3^+$ in the direction of $\zeta$ Persei, a truly classic diffuse cloud with a low average extinction. Moreover, a significant number of other molecules have been detected along the same line of sight ($H_2$, HD, CO, $C_2$, $C_3$, OH, NH, CH, CH$^+$, CN), as have a variety of atoms in assorted stages of ionization (Savage et al. 1977; Snow 1977; Black et al. 1978; Federman 1982; Danks & Lambert 1983; Jura & Meyer 1985; Meyer & Jura 1985; van Dishoeck & Black 1986; van Dishoeck & Black 1989; Meyer & Roth 1991; Felenbok & Roueff 1996; Maier et al. 2001; Adamkovics et al. 2003). The populations of molecular hydrogen in rotational states through $J = 5$ are also known. Indeed, the cloud in front of $\zeta$ Persei was the subject of a classic model by Black et al. (1978) in which many of the then-known abundances were reproduced with a two-phase model with a cold zone (45 K, $n_H = 267$ cm$^{-3}$, 1.3 pc) and a "hot" zone (120 K, $n_H = 100$ cm$^{-3}$, 1.7 pc). Their ionization rate – $\zeta = 2.2 \times 10^{-17}$ s$^{-1}$ – was determined mainly by the OH abundance (see also Hartquist et al. 1978), although it is also consistent with the HD column density. Analysis of OH observations towards $\zeta$ Perseus was performed by Federman et al. (1996) who obtained an ionization rate of $1.7 \times 10^{-17}$ s$^{-1}$. A more detailed series of models for $\zeta$ Persei is given in the comprehensive paper of van Dishoeck & Black (1986; see in particular their Table 11). In these hydrostatic models, labelled A-G, the density-temperature structure is a continuous one, ranging from higher-temperature, lower-density conditions at the cloud edge to lower-temperature, higher-density conditions at the cloud center. For example, model A maintains a fairly constant density of 200 cm$^{-3}$ but goes from a temperature of 120 K at cloud edge to one under 40 K at the cloud center. Cosmic ray ionization rates $\zeta$ are in the range 4–7 $\times 10^{-17}$ s$^{-1}$. Although a reasonable fit to most of the observed data at that time, the

models fail dramatically for $C_3$, where they fall about five orders of magnitude short (Maier et al. 2001). Their large predictions for the $H_3^+$ abundance must also be discounted, since they all contain a very slow rate for the dissociative recombination of $H_3^+$. A smaller discrepancy occurs for CO, which is under-predicted by factors of 2–7. The molecule CH$^+$ is underproduced dramatically, but this species is a special case because, as is well known, it cannot be reproduced with any low-temperature model, but requires a region of high temperature, either caused by a shock or by some type of turbulence or wave propagation (Gredel et al. 2002; Zsargó & Federman 2003; Joulain et al. 1998). Thus, even prior to the detection of the surprisingly large $H_3^+$ abundance, the diffuse cloud towards $\zeta$ Persei had been recognized to be a rather complex region.

The suggestion of McCall et al. (2003) is that their detection of a large abundance of $H_3^+$ in $\zeta$ Persei most likely implies a high ionization rate, presumably caused by low energy cosmic rays since there is not known to be a specially potent X-ray source in the vicinity. These authors did not determine the effect of their suggestion on the calculated abundances for the many other species detected. The idea of a high ionization rate has also been raised recently by Liszt (2003), who argues that a high value of $\zeta$ ($\zeta_H \geq 2 \times 10^{-16}$ s$^{-1}$) is actually needed in diffuse clouds to explain the HD observations, and can be sustained by considering the rapid destruction of protons via recombination with negatively-charged small grains. But what about all of the detailed observations of classic diffuse clouds that appear to be well explained by models including lower ionization rates? The present paper can be thought of as a response to the exciting detection by McCall et al. (2003); here we will concentrate on finding a detailed model for $\zeta$ Persei that can fit to a reasonable degree all of the observed abundances, including that of $H_3^+$.

Our basic idea is that an ionization rate somewhat higher than the standard value must be invoked to explain the high abundance of $H_3^+$ in a classic diffuse cloud, but that this ionization rate cannot be so large as to ruin agreement with the atomic ionic balance for species such as carbon and sulfur as well as with the abundances of OH and HD, which are thought to be sensitive to the value of $\zeta$. Since the production of these latter species depends on the slightly endothermic chemical reactions:

$$H^+ + O \longrightarrow O^+ + H \qquad k = 6 \times 10^{-10}\, e^{-227/T}\, \text{cm}^3\, \text{s}^{-1} \qquad (1)$$

$$H^+ + D \longrightarrow D^+ + H \qquad k = 1 \times 10^{-9}\, e^{-41/T}\, \text{cm}^3\, \text{s}^{-1}, \qquad (2)$$

they are also sensitive to the temperature. The rate coefficients shown are approximate expressions; recent theoretical determinations have been performed by Stancil et al. (1999) and Savin (2002). The temperature dependence is especially acute for OH since the Boltzmann factor in the rate coefficient of the $H^+ + O$ reaction changes strongly in the temperature range of diffuse clouds (e.g. 40–80 K). A low temperature can hinder OH production, although the measurement of different rotational state populations of $H_2$ along the same line of sight constrains the kinetic temperature. Following earlier authors, we require a second, dense phase to explain the observed abundances of $C_2$ and $C_3$. Although tiny in size, this phase also helps

to explain the abundance of CN, and has some importance for the abundances of CO and neutral C. In our model calculations, we assume that the column densities of the two phases are additive. There is both observational (Crawford 2002) and theoretical (Hartquist et al. 2003) evidence for small dense phases; these are likely to be overpressured and probably short-lived.

In addition to the standard diffuse cloud phases, we consider the possibility that a number of MHD shocks along the line of sight can contribute significantly to the H$_3^+$ column density. Such shocks are often invoked to explain large CH$^+$ abundances in diffuse clouds, and they can in principle produce a high abundance of H$_3^+$ if a large ionization rate is assumed. The mechanism involves the conversion of the high abundance of protons produced by cosmic ray ionization into H$_3^+$ through the endothermic reaction

$$H^+ + H_2 \rightarrow H + H_2^+ \quad k = 5.16 \times 10^{-9} e^{-21106/T} \, cm^3 \, s^{-1} \quad (3)$$
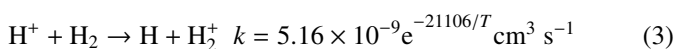
followed by the exothermic reaction between H$_2$ and H$_2^+$. The rate coefficient has been estimated in this work.

The remainder of this paper is organized as follows. In Sect. 2, we discuss our diffuse cloud models and then compare our thermal (non-shock) results with observations for ζ Persei. In Sect. 3, we discuss our MHD shock model, and how the results are constrained by the observed abundance of CH$^+$. Section 4 contains a discussion and a summary of our results.

## 2. Model of ζ Persei and results

We have used an updated version of the PDR cloud model of Le Bourlot et al. (1993), in which the cloud is treated as a diffuse PDR. The actual program, which is explained in Le Petit et al. (2002) and Nehme et al. (in preparation), can be downloaded from the URL `http://aristote.obspm.fr/MIS/`. The PDR model features a plane-parallel slab of gas and dust illuminated on one side by a UV radiation field. Radiative transfer as well as thermal balance are solved, although the temperature can also be fixed, if derived from observations, as is the case here. The *J*-dependent photodissociation of molecules such as H$_2$ and HD as well as their excitation in ro-vibrational levels due to radiative excitation, decay, and collisional excitation are computed. The photodissociation of CO and excitation in its rotational levels are taken into account, as well as the photoionisation and statistical equilibrium in the fine structure levels of C, S and O. An interest of this model is that the photodissociation of H$_2$, HD, CO and the photionization of C are computed in a self-consistent way. About one-hundred chemical species linked by a network of more than one thousand chemical reactions are taken into account.

For our calculations of ζ Persei, we utilized the elemental abundances shown in Table 1 and the parameters listed in Table 2 for the diffuse and dense phases. The parameters chosen lead to our best overall fit to the observations. The diffuse phase has a rather standard total proton hydrogen density $n_H$ of 100 cm$^{-3}$, an incident radiation field intensity of twice the Draine value (Draine 1978), $\chi = 2$, a temperature of 60 K, which lies in between the maximum (75 K) and minimum (45 K) values determined from H$_2$ *J* = 0, 1 abundances, and an ionization rate ζ of $2.5 \times 10^{-16}$ s$^{-1}$, which is in between

**Table 1.** Elemental abundances with respect to total hydrogen.

| Element | Abundance |
|---------|-----------|
| D[1]    | 1.5(−05)  |
| O[2]    | 3.2(−04)  |
| N[3]    | 7.5(−05)  |
| C[4]    | 1.32(−04) |
| S[4]    | 1.86(−05) |
| Si[5]   | 2.9(−05)  |

1 Linsky et al. (1995).
2 Meyer et al. (1998).
3 Meyer et al. (1997).
4 Savage & Sembach (1996).
5 Black et al. (1978).

**Table 2.** Model parameters.

| Parameter | Diffuse Phase | Dense Phase |
|-----------|---------------|-------------|
| $n_H$ (cm$^{-3}$) | 100 | 20000 |
| $\chi$ | 2.0 | 0.5 |
| ζ ($10^{-17}$ s$^{-1}$) | 25 | 25 |
| $T$(K) | 60 | 20 |
| $N$(H$_2$) (cm$^{-2}$) | 4.5(20) | |
| $N$(C$_2$) (cm$^{-2}$) | | 1.9(13) |

the value of $2.2 \times 10^{-17}$ s$^{-1}$ deduced by Hartquist et al. (1978) using OH and HD and the value of $1.2 \times 10^{-15}$ s$^{-1}$ deduced by McCall et al. (2003) using H$_3^+$. The integration proceeds until a column density for H$_2$ of $4.5 \times 10^{20}$ cm$^{-2}$, close to the midpoint of the values measured, is achieved, leading to a length of 4.0 pc and a visual extinction of 0.694. The dense phase has a much higher value for $n_H$ of $2 \times 10^4$ cm$^{-3}$, an incident radiation field of 0.5 the Draine value, the same ζ, and a temperature of 20 K. The length of the dense phase is determined by integrating the column density of C$_2$ to equal its observed value; this determination leads to a very small length of $4.3 \times 10^{-4}$ pc (80 AU). Welty (private communication) has looked into the possibility that with such a small dense component, temporaral variations in CN should have been detected. He concluded that even a 40 AU-thick sheet might be consistent with no variations in the column density. As will be discussed below, the density of both phases is highly constrained by the total column densities of neutral carbon and sulfur atoms. Finally, it is clear from atomic studies that our two-phase model is a simplification. For example, the line of sight towards ζ Persei has been studied in K I by Welty et al. (2001), who detected two main and two weak diffuse components. Our diffuse phase must then be considered as either the sum of these two main components or the more extensive of the two.

The adopted $R_v$ coefficient is 2.8 following Cardelli et al. (1989) and $E(B - V) = 0.32$ (van Dishoeck & Black 1989) giving a ratio of total neutral hydrogen to color excess of $5.2 \times 10^{21}$ atoms cm$^{-2}$ mag$^{-1}$. Without further information, we have adopted the galactic extinction curve as well as the standard properties of dust grains to determine the dust extinction along

**Table 3.** Calculated and observed column densities (cm$^{-2}$) in ζ Persei.

| Species | Diffuse Phase | Dense Phase | Total | Observation | |
|---|---|---|---|---|---|
| H[1] | 3.5(20) | 1.4(17) | 3.5(20) | 5.7(20) | 7.1(20) |
| H$_2$[2] | 4.5(20) | 1.1(19) | 4.6(20) | 3.2(20) | 7.1(20) |
| HD[3] | 1.5(16) | 3.9(13) | 1.5(16) | 2.0(15) | 1.1(16) |
| C$^{+}$[4] | 1.6(17) | 1.2(15) | 1.6(17) | 1.8(17) | |
| C[3] | 1.4(15) | 1.6(15) | 2.8(15) | 2.9(15) | 3.6(15) |
| CO[5] | 3.5(14) | 7.9(13) | 4.2(14) | 5.4(14) | – |
| CH[6] | 2.4(12) | 5.6(12) | 8.0(12) | 1.9(13) | 2.0(13) |
| CH$^{+}$[7] | 2.2(10) | 2.7(08) | 2.2(10) | 3.5(12) | – |
| C$_2$[8] | 1.9(11) | 1.9(13) | 1.9(13) | 1.6(13) | 2.2(13) |
| C$_3$[9] | 3.1(08) | 2.1(12) | 2.1(12) | 1.0(12) | |
| CN[10] | 6.6(10) | 1.9(12) | 1.9(12) | 2.7(12) | 3.3(12) |
| NH[11] | 3.5(11) | 1.2(09) | 3.5(11) | 9.0(11) | – |
| O[12] | 4.0(17) | 7.2(15) | 4.0(17) | 0.2(18) | 1.0(18) |
| OH[13] | 4.9(13) | 1.1(09) | 4.9(13) | 4.0(13) | – |
| H$_3^+$[14] | 2.9(13) | 5.0(09) | 2.9(13) | 8.0(13) | – |
| S$^{+}$[3] | 2.3(16) | 4.1(14) | 2.3(16) | 1.7(16) | 2.3(16) |
| S[3] | 3.7(13) | 1.0(13) | 4.7(13) | 1.5(13) | 2.2(13) |
| Si$^{+}$[3] | 3.6(16) | 6.5(14) | 3.6(16) | 2.8(16) | 6.6(16) |
| H$_2$ ($J = 0$)[2] | 3.0(20) | 1.1(19) | 3.0(20) | 2.2(20) | 4.8(20) |
| H$_2$ ($J = 1$)[2] | 1.5(20) | 1.8(17) | 1.5(20) | 1.0(20) | 2.3(20) |
| H$_2$ ($J = 2$)[3] | 1.9(17) | 4.7(13) | 2.0(17) | 1.1(18) | 2.4(18) |
| H$_2$ ($J = 3$)[3] | 3.9(15) | 2.8(13) | 3.9(15) | 2.0(16) | 9.6(16) |
| H$_2$ ($J = 4$)[3] | 3.0(14) | 2.5(13) | 3.2(14) | 1.1(15) | 2.0(15) |
| H$_2$ ($J = 5$)[3] | 1.2(14) | 8.0(12) | 1.3(14) | 2.3(14) | 2.8(14) |
| Ionization fraction | 2.2(–4) | 1.0(–04) | | | |
| Length | 4.2 pc | 76 AU | | | |
| $A_V$ | 0.69 | 0.013 | 0.70 | | |

1 Bohlin (1975).

2 Savage et al. (1977).

3 Snow (1977) but upper limits reanalyzed here with updated $f$ values (see text) for H$_2$ $J \geq 2$ and for HD using $b = 2.5$ km s$^{-1}$.

4 Cardelli et al. (1996).

5 Snow (1977), with updated $f$-values from van Dishoeck & Black (1986).

6 Jura & Meyer (1985).

7 Federman (1982).

8 Danks & Lambert (1983) – reanalyzed by van Dishoeck & Black (1989).

9 Maier et al. (2001).

10 Meyer & Jura (1985).

11 Meyer & Roth (1991).

12 van Dishoeck & Black (1986).

13 Felenbok & Roueff (1996).

14 McCall et al. (2003).

the line of sight as a function of wavelength. Numerical values can be found in Le Petit et al. (2002), Table 2.

Table 3 shows the observed and calculated column densities for ζ Persei, while Table 4 shows calculated column densities for some undetected species. The observed values are taken from a variety of sources. If more than one observed column density is given, the two values represent lower and upper limits. The case of H$_2$ for rotational levels with $J \geq 2$ merits special attention. Here we have used the average values of Snow (1977) as the lower limit and typically larger values obtained here as the upper limit. The new numbers were obtained with a curve-of-growth analysis based on updated $f$ values (Abgrall et al. 1993, 1994) resulting in a new value of 2.5 km s$^{-1}$ for the Doppler parameter $b$. Because the only observed line of HD in the Copernicus spectrum is located on the flat part of the curve of growth, this new $b$ value also has the effect of increasing significantly the upper limit on N(HD) compared with the value of Snow (1977). The calculated column densities are divided into their diffuse phase and dense phase values. A quick perusal of the rather long Table 3 shows that almost all observed column densities are fit to within a factor of three or better. Below we discuss the agreement for individual species

**Table 4.** Calculated column densities (cm$^{-2}$) in $\zeta$ Persei for undetected species.

| Species | Diffuse Phase | Dense Phase | Total |
|---|---|---|---|
| D | 3.6(15) | 3.0(14) | 3.9(15) |
| Si | 4.0(13) | 9.5(12) | 4.9(13) |
| H$^+$ | 9.6(16) | 1.8(12) | 9.6(16) |
| D$^+$ | 2.5(11) | 3.0(06) | 2.5(11) |
| H$_2^+$ | 1.4(12) | 1.3(08) | 1.4(12) |
| H$_2$D$^+$ | 6.5(09) | 1.2(06) | 6.5(09) |
| OH$^+$ | 7.6(11) | 3.1(06) | 7.6(11) |
| H$_2$O$^+$ | 5.5(11) | 2.9(06) | 5.5(11) |
| H$_3$O$^+$ | 5.2(11) | 4.5(06) | 5.2(11) |



**Fig. 1.** Calculated column density (cm$^{-2}$) of $H_3^+$ as a function of $\zeta$ for diffuse-phase models in which $n_H = 100$ cm$^{-3}$ and $\chi = 2$. The horizontal value is that observed for $\zeta$ Persei.



**Fig. 2.** Calculated column density (cm$^{-2}$) of H$^+$ as a function of $\zeta$ for diffuse-phase models in which $n_H = 100$ cm$^{-3}$ and $\chi = 2$.

and the dependence of calculated column densities on $\zeta$, gas temperature, and the density of the dense phase.

## 2.1. Individual species

### 2.1.1. $H_3^+$

The calculated column density for $H_3^+$, which stems almost entirely from the diffuse phase, is 1/3 of the observed value in $\zeta$ Persei. A plot of the column density vs. $\zeta$ can be seen in Fig. 1. In this and subsequent figures, the calculated column density for the normally dominant diffuse portion is plotted vs. $\zeta \times 10^{17}$ in units of s$^{-1}$, while the horizontal line (or lines) represents the observed abundance. The calculations were performed at three temperatures: 60 K, the temperature of our best fit, and 45 K and 75 K, the lower and the upper limits of the observed temperature $T_{01}$ for the lowest two rotational states of H$_2$. As can be seen in Fig. 1, the column density of $H_3^+$ increases with increasing $\zeta$ and temperature. The direct dependence on ionization rate stems from the fact that the cosmic ray ionization of molecular hydrogen leads directly to the production of $H_3^+$. The temperature dependence, which is more apparent at high $\zeta$, is caused partially by the increasing importance of electrons in the destruction of $H_3^+$ and the inverse temperature dependence ($T^{-0.5}$) of the dissociative recombination. Since we are plotting column density rather than abundance, a simple steady-state formula for concentration does not give the actual dependence. Given the dependence on $\zeta$, one can see how McCall et al. (2003) derived their very high value for this parameter, but in our global fit, we find, as will be brought out below for a variety of species (see Sect. 2.2 below), that there are difficulties with too high an ionization rate. The most direct result of a higher ionization rate is a higher fractional ionization because the proton abundance becomes significantly greater than that of the otherwise dominant ion C$^+$, which is formed through photoionization. The near linear dependence of $N(H^+)$ on $\zeta$ is shown in Fig. 2. A large H$^+$ column density may not be compatible with the absence of radio recombination lines in similar but more distant sources, but the column density of protons can be depleted by collisions with negatively-charged PAH's (Liszt 2003), not considered here.
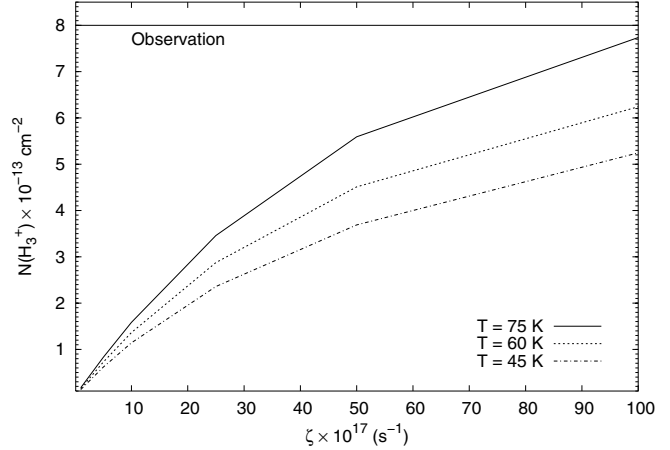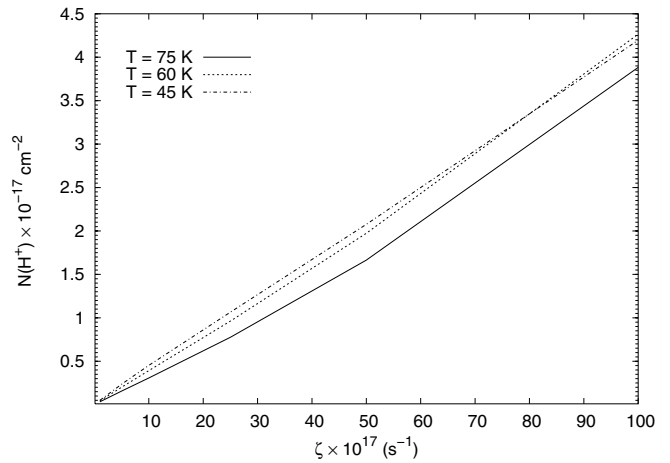
A higher fractional ionization leads to too much neutral C and S (see Fig. 3) through the recombination reactions:

$$C^+ + e^- \longrightarrow C + h\nu \tag{4}$$

$$S^+ + e^- \longrightarrow S + h\nu \tag{5}$$

although a higher radiation field can be invoked to reduce this trend. Note that the problem of neutral C and S is worsened by significant column densities in the dense phase (Table 3).

### 2.1.2. Neutral and ionized atoms

The total calculated column density of neutral C fits the observed value exactly, while that of neutral S is a factor of two to three higher. The former has roughly equal components in the diffuse and dense phases, while the latter has somewhat more in the diffuse phase. These two species are among the most difficult ones to reproduce when one attempts to fit molecular column densities. The ratio $n_H/\chi$ for the dense component needs to be high enough to reproduce $N(C_2)$ and $N(C_3)$ without overestimating $N(C)$ and $N(S)$. The calculated column density of
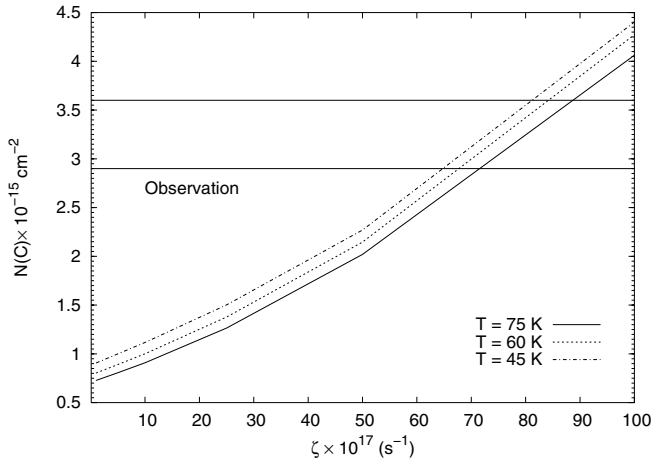
**Fig. 3.** Calculated column density (cm$^{-2}$) of $N$(C) as a function of $\zeta$ for diffuse-phase models in which $n_H$ = 100 cm$^{-3}$ and $\chi$ = 2. The horizontal values are the observed limits for $\zeta$ Persei.



**Fig. 4.** Calculated column density (cm$^{-2}$) of OH as a function of $\zeta$ for diffuse-phase models in which $n_H$ = 100 cm$^{-3}$, and $\chi$ = 2. The horizontal value is that observed for $\zeta$ Persei.

neutral H, stemming overwhelmingly from the diffuse phase, is approximately a factor of two too low, but some of the observed H may well come from the diffuse (WNM) material outside of the cloud and along the line of sight. For example, for a distance of 200 pc ($\zeta$ Per is $\approx$300 pc from the Earth), the average column density for atomic hydrogen can be expected to be 2–3 $\times$ 10$^{20}$ cm$^{-2}$ (Heiles & Troland 2003), which corresponds to a density of approximately 3 H atoms per cubic centimeter.

The discrepancy involving H can also be dramatically lessened by adopting a model in which the radiation field strikes the cloud at both ends, so that one integrates the molecular hydrogen column density from an end to the middle, and then multiplies the result by a factor of two (van Dishoeck & Black 1986). We then obtain a column density of 5.8 $\times$ 10$^{20}$ cm$^{-2}$ for atomic H, which lies in between the measured lower and upper limits. Performing the integration in this manner does not change most of the other results substantially except for OH and CO.

The calculated large abundances of C$^+$ and S$^+$, stemming from the diffuse phase, are in reasonable agreement with observation, which is not surprising since they are mainly determined by the elemental abundances for carbon and sulfur utilized.

The column density of protons in our model is approximately one-half of the carbon ion column density. Whether this amount of HII is detectable via recombination lines (Liszt 2003) is not clear to us.

### 2.1.3. O and OH

The calculated O column density is in the errorbars. OH arises in the diffuse phase from an ion-molecule chain of reactions starting with the O$^+$ ion, produced by reaction (1). Since it is endothermic, this reaction is aided by an increase in temperature. In addition, the larger $\zeta$, the greater the production of H$^+$ so that the more OH is produced. Thus, the dependence of $N$(OH) on $\zeta$, as depicted in Fig. 4, comes as no surprise
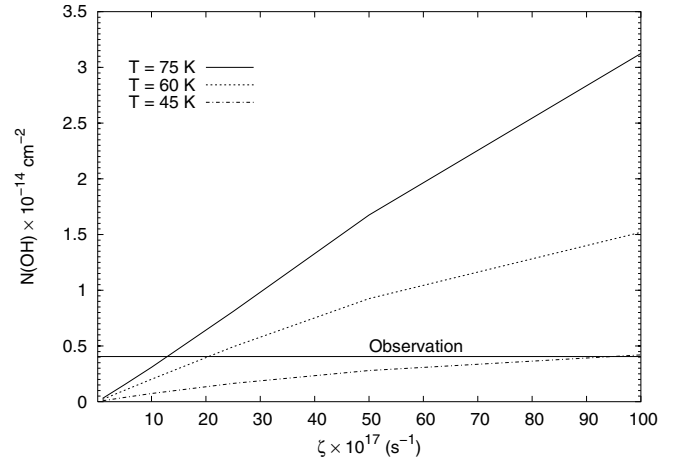
(Le Petit et al. 2002). An ionization rate of 10$^{-15}$ s$^{-1}$ will result in much too high a value of $N$(OH) unless the temperature is lower than normally considered for classical diffuse clouds such as $\zeta$ Persei. With the ionization rate and temperature chosen for our model of this source, the calculated OH column density is very close to the observed value. The temperature chosen for the diffuse portion of their cloud by Black et al. (1978) is 120 K; at this high a temperature, the OH production is far more efficient and requires a lower value of $\zeta$.

### 2.1.4. HD

The isotopomer HD is produced from D$^+$ via the rapid exothermic reaction:

$$D^+ + H_2 \longrightarrow HD + H^+. \tag{6}$$

Although the production of D$^+$ is weakly endothermic, the dependence on temperature is minimal above a value in excess of the endothermicity (42 K). Thus, Fig. 5 shows little temperature dependence for the HD column density in the 45–75 K range. In addition, this figure illustrates that there is only a minimal dependence on $\zeta$ above 10$^{-16}$ s$^{-1}$. This minimal dependence contrasts with earlier models that used lower values of $\zeta$ (Hartquist et al. 1978) because HD tends to be self-shielded and destroyed by ionic reactions (Le Petit et al. 2002). In particular, with the chosen parameters (e.g. $T$ = 60 K), the transition D/HD occurs at $A_v$ = 0.1 so the photodissociation of HD throughout much of the diffuse phase is inefficient. This very small visual extinction at which the D/HD transition takes place is due to an enhancement of the formation rate of HD by the high flux of cosmic rays.

The total column density we calculate for HD is up to a factor of 8 larger than what is detected. This result is almost independent of the $\zeta$ chosen once values much larger than 10$^{-17}$ s$^{-1}$ are adopted. Some of the discrepancy can be mitigated by adopting a somewhat lower D/H elemental abundance ratio. If one decreases the D/H ratio in the diffuse component by a factor of 2, the resulting $N$(HD) is 6.4 $\times$ 10$^{15}$ cm$^{-2}$ ($T$ = 60 K, $\zeta$ = 25 $\times$ 10$^{-17}$ s$^{-1}$), which is below the level of the observed
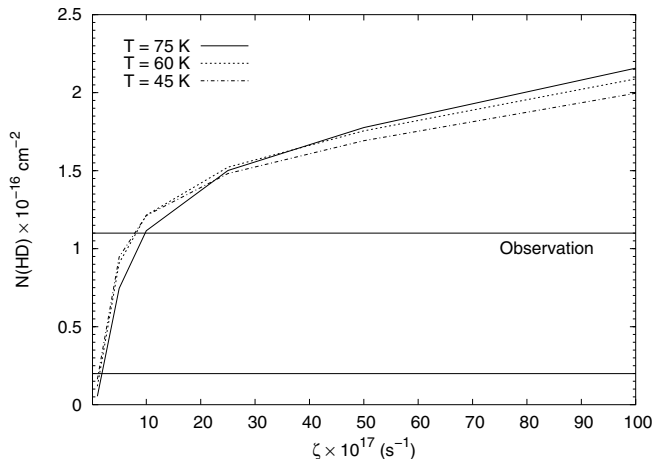
**Fig. 5.** Calculated column density (cm$^{-2}$) of HD as a function of $\zeta$ for models in which $n_H = 100$ cm$^{-3}$ and $\chi = 2$. The horizontal values are the lower and upper limits to the observed values for $\zeta$ Persei.

upper limit. As a reminder, the lines used to determine $N$(HD) in the Copernicus spectrum by Snow (1977) are saturated and so $N$(HD) is highly dependent on the Doppler parameter $b$ utilized. The upper limit in the table comes from our latest analysis, and is equal to the calculated value.

### 2.1.5. NH

Originally thought to be produced only by grain-surface reactions, this species is now known to be synthesized in the gas phase, starting with the reaction between N$^+$ and ortho-H$_2$ (Le Bourlot 1991), which has enough energy to overcome the small reaction endothermicity. The ionization of nitrogen atoms is caused directly by cosmic rays while NH is mainly depleted by photodissociation. So, one expects a direct correlation between $N$(NH) and $\zeta$, a dependence which is indeed found to be the case. Our calculated column density of NH is within a factor of three of the observed amount; it is overwhelmingly located in the diffuse phase.

### 2.1.6. CO, CN, C$_2$, C$_3$

In the current model, CO is produced in both the diffuse and dense phases, with the diffuse cloud component approximately four times that of the dense cloud. Our total column density is very close to the observed value. The dependence of the calculated CO column density on $\zeta$ closely follows that of OH because the main formation reaction of CO is C$^+$ + OH.

Our model predicts a column density for CN that is approximately 1/2 of the observed value, but it all is to be found in the small dense phase. The need to form CN under denser conditions than our diffuse phase has been discussed recently by Gredel et al. (2002). Our current network does not contain the reaction between C$_2$ and N to form CN and C (Federman, private communication). Inclusion of this reaction does not significantly affect our results.

The species C$_2$ and C$_3$, for which our model results are in excellent agreement with observation, derive from the dense

phase of our two-phase model cloud. Recent studies of both the abundance of C$_2$ and its rotational distribution are somewhat ambivalent about what densities are needed to best reproduce C$_2$. Cecchi-Pestellini & Dalgarno (2002) favor a density of 600 cm$^{-3}$ while the same authors (Cecchi-Pestellini & Dalgarno 2000), in an earlier paper, mention significantly higher densities. According to the recent study of Adamkovics et al. (2003), the density needed to reproduce best the rotational distribution of C$_2$ is 460 ± 150 cm$^{-3}$, significantly lower than our value of $2 \times 10^4$ cm$^{-3}$. In the models of van Dishoeck & Black (1986), the C$_2$ abundance is also reproduced at significantly lower densities. Part of the discrepancy stems from their use of a much higher elemental carbon abundance, but part must also stem from differences in the chemistry. To determine the effect of a much lower density in our dense phase, we integrated through the phase to produce the lower detected limit of C$_2$ as a function of density. At a density of 500 cm$^{-3}$, we find other molecules, most significantly H$_2$, and the neutral atoms C and S to be overabundant by a considerable extent. We then looked carefully at the C$_2$ excitation problem and found that the higher density we use does not seriously worsen the agreement with the observational rotational distribution; the problem of an overly large $J = 6$ abundance remains (see the C$_2$ calculator of McCall at `http://dibdata.org`).

### 2.1.7. H$_2$ rotational populations

Unlike the case of C$_2$, our model considers the rotational populations of molecular hydrogen. The details of our approach are to be found in Le Petit et al. (2002). Overall, our model is in excellent agreement with observation for $J = 0, 1$, but underproduces H$_2$ for $J = 2–5$. The cold dense component is of no importance for any $J$ considered. The contribution of one or more MHD shocks along the line of sight is discussed in the next section. We have also checked the dependence of the rotational excitation on the formation mechanism of H$_2$. The scenario used in our model assumes equipartition among the different degrees of freedom, so that the internal excitation of newly formed molecular hydrogen corresponds to a temperature of about 17 000 K (1.5 eV). This internal excitation is divided statistically among vibration-rotation levels. Two other scenarios have been discussed in Black & van Dishoeck (1987) corresponding to rotationally cold and vibrationally hot H$_2$. We have run models with such assumptions and found that the excitation of H$_2$ was significantly reduced for levels with $J$ larger than 3.

### 2.2. A high ionization rate

What happens if we adopt an ionization rate $\zeta$ equal to that chosen by McCall et al. (2003) with the same physical conditions used in our model? Although the H$_3^+$ abundance can be fit exactly (see Fig. 1), the following species are over produced in the diffuse component by the factors listed in parenthesis: OH(4), CO(4), S(6), C(1.4). The factors of 4–6 are considerably larger than those obtained with our favored model. Improved agreement for OH and CO can be obtained by lowering the temperature to below 50 K, but this will have a negative impact on

**Table 5.** Column densities (cm$^{-2}$) from assorted MHD shock calculations applied to $\zeta$ Persei.

| Species | 1 shock $v = 11$ km s$^{-1}$ | 9 shocks $v = 8$ km$^{-1}$ | 3 shocks $v = 9$ km$^{-1}$ | Observation |
|---|---|---|---|---|
| CO | 2.1(12) | 5.2(12) | 2.2(12) | 5.4(14) |
| CH | 1.1(12) | 3.0(12) | 6.7(12) | 2.0(13) |
| CH$^+$ | 4.0(12) | 3.0(12) | 3.9(12) | 3.5(12) |
| C$_2$ | 1.1(10) | 3.4(10) | 6.6(10) | 1.9(13) |
| C$_3$ | 9.8(6) | 2.5(7) | 1.7(7) | 1.0(12) |
| CN | 4.6(10) | 4.9(10) | 5.2(10) | 3(12) |
| NH | 7.9(9) | 4.9(8) | 1.4(9) | 9.0(11) |
| OH | 1.3(13) | 1.7(13) | 1.1(13) | 4.0(13) |
| H$_3^+$ | 1.3(12) | 3.4(11) | 1.4(11) | 8.0(13) |
| H | 1.5(18) | 1.4(19) | 9.5(18) | 6.2(20) |
| H$_2$ | 7.2(17) | 6.3(18) | 4.4(18) | 4.6(20) |
| H$_2$ ($J = 0$) | 1.4(17) | 1.5(18) | 8.9(17) | 3.5(20) |
| H$_2$ ($J = 1$) | 3.6(17) | 3.6(18) | 2.9(18) | 1.6(20) |
| H$_2$ ($J = 2$) | 9.5(16) | 7.6(17) | 4.6(17) | 2.4(18) |
| H$_2$ ($J = 3$) | 1.1(16) | 4.0(17) | 1.6(17) | 9.6(16) |
| H$_2$ ($J = 4$) | 6.4(15) | 1.1(16) | 3.9(15) | 2.0(15) |
| H$_2$ ($J = 5$) | 1.8(15) | 1.1(15) | 3.6(14) | 2.8(14) |
| Length (pc) | 0.028 | 0.25 | 0.074 | |
| $A_v$ | 0.015 | 0.14 | 0.036 | |

the column densities of H$_3^+$, NH, S, and C. Improved agreement with S and C can be obtained by enhancing the radiation field but then molecules will be photodissociated. Finally, the large abundance o HII probably implies that a detection via recombination spectra is possible, although Liszt (2003) has suggested that such an abundance can be reduced by consideration of charge neutralization on small grains. In summary, a value for $\zeta$ that is enhanced over the classical value by an order of magnitude but not by a much greater factor seems to be a reasonable compromise for fitting all of the observed abundances. Of course, the agreement between observation and theory for the various species cannot approach that obtained in earlier approaches where a smaller number of observations were fit.

Models with thermal balance included show that an increase in the ionization rate to $25 \times 10^{-17}$ s$^{-1}$ does not modify the kinetic temperature. Because of the small visual extinction in both the diffuse and dense components, heating is dominated by photoelectric processes on grains.

## 3. The CH$^+$ constraint and shock models

The ion CH$^+$ was detected towards $\zeta$ Persei by Federman (1982). Its column density has been re-estimated by van Dishoeck & Black (1986) and found to be $3.5 \times 10^{12}$ cm$^{-2}$. It is well known that standard quiescent diffuse cloud models are not able to produce CH$^+$ in sufficient amounts because the main formation reaction of this ion involves the endothermic reaction between C$^+$ and H$_2$, with a sizeable endothermicity of 4250 K. Various mechanisms have been proposed to provide the necessary energy input; MHD shocks offer a plausible hypothesis to explain the observed abundance of CH$^+$, as discussed by Flower & Pineau des Forêts (1998). Such shocks can also enhance H$_3^+$ formation via the endothermic reaction H$^+$ + H$_2$ → H$_2^+$ + H, which is followed by the rapid

reaction between H$_2^+$ and H$_2$, giving H$_3^+$ + H. However, the endothermicity of the H$^+$ + H$_2$ reaction (reaction (3)) is over 20 000 K, which is much larger than the one involved in the production of CH$^+$.

We have run an MHD shock model developed for the HD 34078 line of sight (Boissé et al., in preparation) in which the excitation of H$_2$ is taken into account. We have also run various shock models with lower velocity, following the idea developed by Gredel et al. (2002) that several shocks could be present along the line of sight. The idea is to attempt to find parameters that result in a column density of CH$^+$ close to the observed value and to determine whether such shocks can also produce sufficient amounts of H$_3^+$. In our calculations, we have calculated reverse (endothermic) reaction rate coefficients by assuming a quasi- thermal equilibrium in which rotation is treated classically while vibration is assumed to be unexcited. The rate coefficients are available upon request. Our calculated column densities for three models are displayed in Table 5 along with observed values. The three models are: (a) one shock with $v = 11$ km s$^{-1}$, (b) nine shocks with $v = 8$ km s$^{-1}$, and (c) three shocks with $v = 9$ km s$^{-1}$. In all models, $B = 5.3$ $\mu$Gauss. The observed column densities for $\zeta$ Persei listed in this table are averages in the cases where lower and upper limits exist, except for H$_2$ ($J \geq 2$), where we have used our new column densities calculated with a $b$ value of 2.5 km s$^{-1}$.

A glance at Table 5 shows that all three shock models reproduce the column density of CH$^+$ accurately. However the amount of H$_3^+$ is far from sufficient by itself to explain the observed abundance; indeed, it is less than 10% of the observed column density even for the best case (the single shock). If the shock velocities are increased to enlarge the calculated abundance of H$_3^+$, the amount of CH$^+$ calculated becomes much too

large. So, shock models do not appear to be a panacea for the production of the H$_3^+$ ion.

What about the other predictions of the shock models? For most species, the column densities in the shocks are not significant. Even for OH, the amount in our two-phase model is 3–4 times that in the shocks. But the shocks are important, indeed critical, for the overall populations of excited rotational levels of H$_2$. While our thermal two-phase model underproduces H$_2$ for $J = 2-5$, it can be seen in Table 5 that the assorted shock models add considerably to the column density for rotational levels with $J \geq 2$. The best model appears to be the one with 3 shocks. Specifically, the ratio between the observed and calculated H$_2(J)$ column densities for the thermal + 3-shock model are 3.6, 0.60, 0.50, and 0.57 if our new H$_2$ column densities are used, and 1.7, 0.13, 0.26, and 0.47 if average values of Snow (1977) are used for $J = 2, 3, 4, 5$, respectively.

## 4. Discussion

The new observation by McCall et al. (2003) that there is a large column density of H$_3^+$ in the classic diffuse cloud towards $\zeta$ Persei raises a serious problem since the result was not predicted by models of this reasonably well-understood cloud. Previous detections of large abundances of H$_3^+$ in the diffuse interstellar medium (Geballe et al. 1999; McCall et al. 2002) were not directed at close, presumably well-understood sources. If one only wishes to fit the observed column density of H$_3^+$, this can be done by invoking a very large path length or a very high cosmic ray-induced ionization rate, or some combination of the two. McCall et al. (2003) prefer a standard path length (2.1 pc) and a very high ionization rate $\zeta$ of $1.2 \times 10^{-15}$ s$^{-1}$. But what about all of the other atoms and molecules detected along this line of sight, and reasonably fit to a model with a much lower ionization rate?

Using a detailed PDR model for the diffuse cloud in the direction of $\zeta$ Persei, we have attempted to find the best fit to all observations, including that of H$_3^+$. We have found that a cloud with three phases is required, an MHD shock phase or phases to fit the abundance of CH$^+$ and to help with the abundances of rotationally excited H$_2$, a small thermal dense phase mainly for CN, C$_2$, and C$_3$, and a large diffuse cloud (4.2 pc in length). An ionization rate of $2.5 \times 10^{16}$ s$^{-1}$ seems to be a good compromise between the need for a higher rate, which would fit the H$_3^+$ abundance better, and a lower rate, which would fit S and possibly HD better.

With the chosen physical parameters and a model consisting of the two thermal phases plus three MHD shocks, we are able to come within a factor of 3 or better for all observed abundances, with the possible exceptions of HD, and H$_2$ ($J = 2$), where the issue is complicated by the accuracy of the observed column densities. Whether or not our results can be improved by the adoption of a model with continuous variation in density and temperature in place of two thermal phases is unclear at this stage; it does appear that our small high density clump is critical.

If an ionization rate significantly larger than the classical value of $1-5 \times 10^{-17}$ s$^{-1}$ is really correct, then there is the question of what causes it. One can speculate on whether our high

value of $\zeta$ comes from a particularity of the line of sight towards $\zeta$ Persei, or as is more likely considering the detection of large amounts of H$_3^+$ elsewhere, the standard value of $\zeta$ is underestimated, at least in diffuse regions. The suggestion that low energy cosmic rays (2–50 MeV per nucleon) exist at the edge of the solar system based on Voyager and Pioneer observations (Weber 1998) supports the contention that enhanced ionization rates are widespread in regions with weak magnetic field and due to low energy cosmic rays. The analysis of other lines of sight should help to clarify this point. It would also be useful to confirm the high ionization rate we infer by checking some predictions that come from it. For example, a look at Table 4 shows that predictions for the abundances of the ions OH$^+$, H$_2$O$^+$, and H$_3$O$^+$ are all in the $10^{12}$ cm$^{-2}$ range, which might allow detection.

## References

Abgrall, H., Roueff, E., Launay, F., Roncin, J.-Y., & Subtil, J. L. 1993, J. Mol. Spec., 157, 512
Abgrall, H., Roueff, E., Launay, F., & Roncin, J.-Y. 1994, Can. J. Phys., 72, 856
Adamkovics, M., Blake, G. A., & McCall, B. J. 2003, ApJ, 595, 235
Amano, T. 1988, ApJ, 329, L21
Black, J. H. 2000, Phil. Trans. Roy. Soc. London A, 358, 2515
Black, J. H., & van Dishoeck, E. F. 1987, ApJ, 322, 412
Black, J. H., Hartquist, T. W., & Dalgarno, A. 1978, ApJ, 224, 448
Bohlin, R. C. 1975, ApJ, 200, 402
Cardelli, J. A., Clayton, G. C., & Mathis, J. S. 1989, ApJ, 345, 245
Cardelli, J. A., Meyer, D. M., Jura, M., & Savage, B. D. 1996, ApJ, 467, 334
Cecchi-Pestellini, C., & Dalgarno, A. 2000, MNRAS, 313, L6
Cecchi-Pestellini, C., & Dalgarno, A. 2002, MNRAS, 331, L31
Crawford, I. A. 2002, MNRAS, 334, L33
Dalgarno, A., & McCray, R. A. 1972, ARA&A, 10, 375
Danks, A. C., & Lambert, D. L. 1983, A&A, 124, 188
Draine, B. 1978, ApJS, 36, 595
Federman, S. R. 1982, ApJ, 257, 125
Federman, S. R., Weber, J., & Lambert, D. L. 1996, ApJ, 463, 181
Felenbok, P., & Roueff, E. 1996, ApJ, 465, 57
Flower, D. R., & Pineau des Forêts, G. 1998, MNRAS, 297, 1182
Geballe, T. R., & Oka, T. 1996, Nature, 384, 334
Geballe, T. R., McCall, B. J., Hinkle, K. H., & Oka, T. 1999, ApJ, 510, 251
Gredel, R., Pineau des Forêts, G., & Federman, S. R. 2002, A&A, 389, 993
Hartquist, T. W., Black, J. H., & Dalgarno, A. 1978, MNRAS, 185, 643
Hartquist, T. W., Falle, S. A. E. G., & Williams, D. A. 2003, Ap&SS, 288, 369
Heiles, C., & Troland, T. H. 2003, ApJ, 586, 1067
Herbst, E. 2000, Phil. Trans. Roy. Soc. London A, 358, 2523
Herbst, E., & Klemperer, W. 1973, ApJ, 185, 505

Joulain, K., Falgarone, E., Pineau des Forêts, G., & Flower, D. 1998, A&A, 340, 241

Jura, M., & Meyer, D. M. 1985, ApJ, 294, 238

Kokoouline, V., & Greene, C. H. 2003, PhRvL, 90, 13320-1

Larsson, M. 2000, Phil. Trans. Roy. Soc. London A, 358, 2433

Larsson, M., Danared, H., Mowat, J. R., et al. 1993, PhRvL, 70, 430

Le Bourlot, J. 1991, A&A, 242, 235

Le Bourlot, J., Pineau des Forêts, G., Roueff, E., & Flower, D. 1993, A&A, 267, 233

Le Petit, F., Roueff, E., & Le Bourlot, J. 2002, A&A, 390, 369

Liszt, H. 2003, A&A, 398, 621

Linsky, J. L., Diplas, A., Wood, B. E., et al. 1995, ApJ, 451, 335

Maier, J. P., Lakin, N. M., Walker, G. A. H., & Bohlender, D. A. 2001, ApJ, 553, 267

McCall, B. J., Geballe, T. R., Hinkle, K. H., & Oka, T. 1999, ApJ, 522, 338

McCall, B. J., Hinkle, K. H., Geballe, T. R., et al. 2002, ApJ, 567, 391

McCall, B. J., Huneycutt, A. J., Saykally, R. J., et al. 2003, Nature, 422, 500

Meyer, D. M., & Jura, M. 1985, ApJ, 297, 119

Meyer, D. M., & Roth, K. C. 1991, ApJ, 376, L49

Meyer, D. M., Cardelli, J. A., & Sofia, U. J. 1997, ApJ, 490, L103

Meyer, D. M., Jura, M., & Cardelli, J. A. 1998, ApJ, 493, 222

Nehme, C., Le Petit, F., Hilly-Blant, P., Le Bourlot, J., & Roueff, E., A&A, in preparation

Plasil, R., Glosik, J., Poterya, V., et al. 2003, in Dissociative Recombination of Molecular Ions with Electrons, ed. S. L. Guberman (Dordrecht: Kluwer), 249

Savage, B. D., Drake, J. F., Budich, W., & Bohlin, R. C. 1977, ApJ, 216, 291

Savage, B. D., & Sembach, K. R. 1996, ARA&A, 34, 279

Savin, D. W. 2002, ApJ, 566, 599

Snow, T. P. 1977, ApJ, 216, 724

Solomon, P. M., & Werner, M. W. 1971, ApJ, 165, 41

Stancil, P. C., Schultz, D. R., Kimura, M., et al. 1999, A&AS, 140, 225

van Dishoeck, E. F., & Black, J. H. 1986, ApJS, 62, 109

van Dishoeck, E. F., & Black, J. H. 1989, ApJ, 340, 273

Weber, W. R. 1998, ApJ, 506, 329

Welty, D. E., & Hobbs, L. M. 2001, ApJS, 133, 345

Zsargó, J., & Federman, S. R. 2003, ApJ, 589, 319